# Galaxy rotation

Andrzej Novak

September 1, 2016

**Abstract**

In this paper, the rotational curve of Milky Way is obtained, by measuring the Doppler shift of the 21 cm hydrogen emission line. Two models are fitted to the data to show that purely Keplerian description is insufficient and a more complex approach, involving dark matter, is necessary. Based on two separate measurements the value obtained for the mass of the baryonic matter is $M_B = 1.74 \pm 0.53 \times 10^{10} M_\odot$ and the value for the mass of the dark matter, within a scale radius is $M_s = 1.34 \pm 0.11 \times 10^{11} M_\odot$.

# 1 Introduction

Galactic rotation has proved surprisingly non-trivial. The first to notice that stellar movement deviates from the predictions based on visible (baryonic) matter was Jan H. Oort [6] in 1932. In 1944 van de Hulst [7] predicted a way to measure the rotational speed of Milky Way, using a particular hydrogen spectral line, unaffected by the stellar dust. A successful profile for the hypothesized dark matter was proposed in 1996 by Navarro, Frenk and White [1]. Description of current knowledge on the galactic rotation of Milky Way can be found in McMillan [5] (2011).

The importance of measuring the rotational velocity of the galaxy lies in providing experimental evidence for the existence of dark matter. This paper employs the model profile proposed by Navarro, Frenk and White (NFW profile) and the measurement technique proposed by van de Hulst.

# 2 Theory

This paper considers two models for the rotational velocity of the Milky Way, a purely Keplerian one, which only considers baryonic matter, and a combined model with elements of baryonic and dark matter.

## 2.1 Model 1 - Baryonic Matter

The first model in Equation (3) assumes that Milky Way consists only of visible (baryonic) matter and is Keplerian in that it assumes mass to be concentrated in the

centre of rotation. It is derived by balancing the gravitational and the centripetal force in Equations (1) and (2).

$$F_{centripetal} = F_g \tag{1}$$

$$m\frac{v^2}{R} = \frac{GMm}{R^2} \tag{2}$$

$$v_r(R) = \sqrt{\frac{GM_{Baryonic}}{R}} \tag{3}$$

This model has limitations, but it is used, because most baryonic matter is contained within the galactic radius of 4 kpc [2]. Measurements of velocity outside this radius can be modelled with the approximation that all mass is concentrated in the centre.

## 2.2 Model 2 - Baryonic and Dark Matter

The second model considered in Equation (4) combines the baryonic component with a dark matter component in Equation (5), and assumes that dark matter is distributed as a function of radius $R$.

$$v_r(R) = \sqrt{\frac{G(M_{Baryonic} + M_{Dark}(R))}{R}} \tag{4}$$

$$M_{Dark}(R) = \int_0^R 4\pi r^2 \rho(r) dr \tag{5}$$

Here, $\rho(r)$ is the density profile from the NFW profile [1] and is dependent on two scale parameters: $R_s$, the scale radius and $\rho_0$, the dark matter density normalization, as shown in Equation (6).

$$\rho(r) = \frac{\rho_0}{\frac{r}{R_s}(1+\frac{r}{R_s})^2} \tag{6}$$

By combining Equations (5) and (6), an expression for the mass of the dark matter within the radius $R$ is obtained in Equation (7).

$$M_{Dark}(R) = 4\pi\rho_0 R_s^3 \left[ \ln\left(\frac{R_s + R}{R_s}\right) - \frac{R}{R_s + R}\right] \tag{7}$$

The expression in Equation (7) can be simplified by considering the dark matter mass $M_s$, within the scale radius $R_s$ in Equation (8).

$$M_s = 4\pi\rho_0 R_s^3 \left[ \ln\left(\frac{R_s + R_s}{R_s}\right) - \frac{R_s}{R_s + R_s}\right] = 4\pi\rho_0 R_s^3 \left[ \ln(2) - \frac{1}{2}\right] \tag{8}$$

By combining Equations (7) and (8), the final expression for the dark matter component is obtained in Equation (9), as a function of $M_s$ and $R$.

$$M_{Dark}(M_s, R) = \frac{M_s}{[\ln(2) - \frac{1}{2}]} \left[ \ln\left(\frac{R_s + R}{R_s}\right) - \frac{R}{R_s + R}\right] \tag{9}$$

Model 2 is then expressed in Equation (10) as a function of $R$ with parameters $M_B$ for baryonic mass and $M_s$ for dark matter mass within the scale radius $R_s$.

$$v_r(R) = \sqrt{\frac{G(M_{Baryonic} + M_{Dark}(R, M_s))}{R}} \tag{10}$$

# 3 Experimental Apparatus

Interstellar gas in the Milky Way is largely composed of neutral hydrogen atoms. These atoms, consisting of a single proton and a single electron, can be in two quantum spin states: parallel $\left|m_p = \frac{1}{2}, m_e = \frac{1}{2}\right\rangle$ and anti-parallel $\left|m_p = \frac{1}{2}, m_e = \frac{-1}{2}\right\rangle$. When hydrogen transitions from the more energetic parallel to the anti-parallel configuration, it emits a photon of wavelength 21 cm [7]. Due to the Doppler effect, a shift of this spectral line can be observed, which depends on the relative velocity of the Solar System and the observed gas. By measuring this shift, it is possible to obtain the relative velocity.

$$v_{LoS} = -\frac{f_{obs} - f_H}{f_H} c \tag{11}$$

Here $v_{LoS}$ is the relative velocity of the gas to the observer along the line of sight, $c$ is the speed of light, $f_{obs}$ is the measured frequency, and $f_H$ is the original frequency of the emission line.

The measurement is done using the Small Radio Telescope (SRT) developed by Haystack Observatory. The SRT operates by amplifying the potential collected at the focus of the reflective dish (antenna). For more details and in-depth description of how a radio telescope works, consult the SRT manual [8]. A sample measurement is shown in the Appendix, Figure 6.

A correction is needed for the movement of Sun and Earth [9]. This process is managed internally by the employed software [8], which enables directly reading the corrected maximum relative velocity along the line of sight. The rotational velocity of the source is then obtained by taking into consideration the orbital motion of the local standard of rest (LSR).

$$v_r(R) = v_{LSR}(\max) + V_0 \sin(l) \tag{12}$$

$$R = R_0 \sin(l) \tag{13}$$

Here, $v_r(R)$ is the rotational speed at a radius away from the galactic center, $v_{LSR}$ is the measured corrected relative velocity, $V_0$ is the velocity of LSR, $R_0$ is the galactocentric radius of LSR, and $l$ is the galactic longitude. For a schematic of the derivation see the Appendix, Figure 7.

# 4 Data

Two sets of data are collected on different days, at different times for 9 values of galactic length between 10° and 90°. Each measurement is obtained by averaging the spectrum for 5 minutes. However, values for radii within 4 kpc, cannot be well modelled due to the approximation used for baryonic matter. Measured values are shown in Figure 1. Only measurements between 30° and 80° are considered, as the values for rotational velocity close to the centre are also difficult to measure due to significant noise, and because the value measured at $l = 90°$ is unreliable as it measures gas contained within the LSR, against which the corrections are calculated.

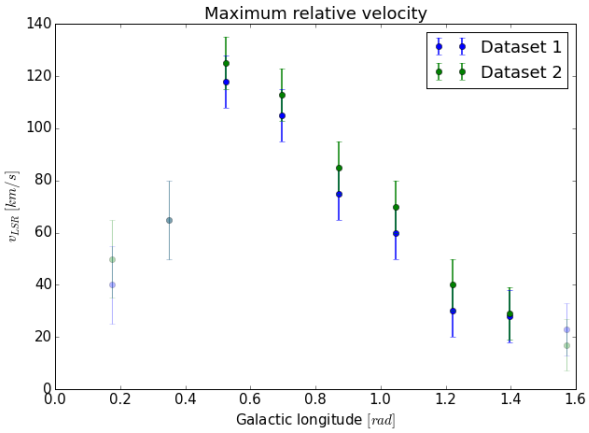


Figure 1: Measurements. Dataset 1 was collected on 4/22/2016, between 8:00 and 9:00. Datset 2 was collected on 4/27/2016, between 7:00 and 9:00. Unused data is greyed out.

The rotational velocity of the hydrogen gas is calculated, using Equation (12) and both models are fitted to the data in Figures 2 and 3, using input parameters in Table 1.

| Variable | Value |
|---|---|
| $R_0$ $[kpc]$ | 8 |
| $V_0$ $[km/s]$ | 220 |
| $R_S$ $[kpc]$ | 10 |
| $G$ $[kpcM_{\odot}^{-1}(km/s)^2]$ | $4.3 \times 10^{-6}$ |

Table 1: Used values and constants. Input parameters used to fit models to the data, in order to estimate the masses of baryonic and dark matter [1] [3] [9].

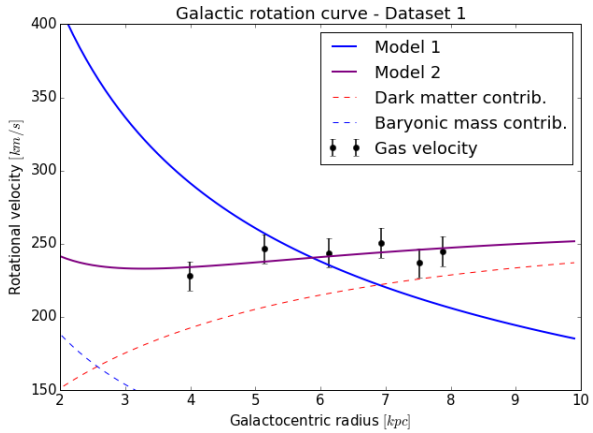


Figure 2: Fitting experimental data. Dataset 1. It is clearly visible that the purely Keplerian description in Model 1 is not sufficient.

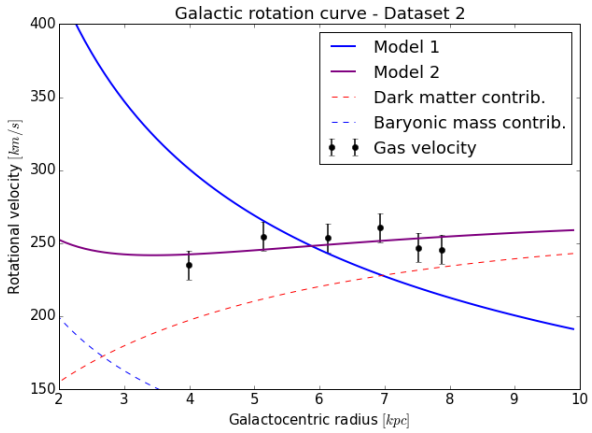


Figure 3: Fitting experimental data. Dataset 2.

The two models are fitted, such that $\chi^2$ of the fits is minimized, which is done by the Levenberg-Marquardt [10] method. The models have different number of degrees of freedom and therefore cannot be compared directly on the basis of $\chi^2$, but instead have to be compared based on their respective probabilities (PTE's) in Table 2.

| | $\chi^2$ | $\chi^2$ probability (PTE) |
|---|---|---|
| Model 1 | 70.00 | $1.03^{-13}$ |
| Model 2 | 2.47 | 0.65 |

(a) Dataset 1.

| | $\chi^2$ | $\chi^2$ probability (PTE) |
|---|---|---|
| Model 1 | 73.08 | $2.34^{-14}$ |
| Model 2 | 3.51 | 0.48 |

(b) Dataset 2.

Table 2: Goodness of fits. $\chi^2$ probabilities of Model 1 are very low, implying that it is extremely unlikely the model is correct for the data. $\chi^2$ probabilities of Model 2 are well within the expected range.

It is clear, from both the fits in Figures 2 and 3 and the $\chi^2$ probabilities in Table 2, that Model 1 is not a viable way to model the data and thus, it is not considered further. The fitted parameters and uncertainties for Model 2 are shown in Table 3.

| Dataset | $M_B[M_\odot]$ | $\sigma_{M_B}[M_\odot]$ | $M_s[M_\odot]$ | $\sigma_{M_s}[M_\odot]$ |
|---|---|---|---|---|
| Dataset 1 | $1.65 \times 10^{10}$ | $0.74 \times 10^{10}$ | $1.31 \times 10^{11}$ | $0.16 \times 10^{11}$ |
| Dataset 2 | $1.84 \times 10^{10}$ | $0.76 \times 10^{10}$ | $1.38 \times 10^{11}$ | $0.16 \times 10^{11}$ |

Table 3: Fitted parameters. Estimates of the mass of baryonic matter $M_B$ and the mass of the dark matter $M_s$, within the scale radius $R_s$ are obtained from the fit of Model 2.

# 5 Results

A consistency check is conducted in Figure 4 for both parameters by comparing the absolute difference of obtained values to zero, within their combined standard deviation $\sigma = \sqrt{\sigma_1^2 + \sigma_2^2}$.

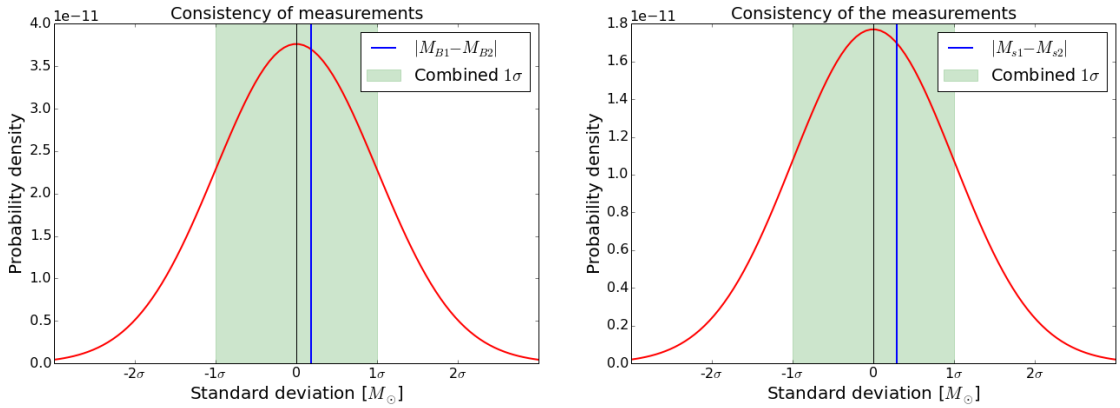


(a) Baryonic component $M_B$.

(b) Dark matter component $M_s$.

Figure 4: Consistency. The absolute differences of measurements obtained from the two datasets are within their respective combined standard deviations from 0 and therefore it can be said that the measurements are consistent.

Since the measurements are consistent, final results are obtained through weighted means of the values obtained from the two datasets by Equation (14) for each mass.

$$M = \frac{\sum_{i=1,2} M_i \sigma_{Mi}^{-2}}{\sum_{i=1,2} \sigma_{Mi}^{-2}} \qquad \sigma_M^2 = \frac{1}{\sum_{i=1,2} \sigma_{Mi}^{-2}} \tag{14}$$

This yields the final values of $M_B = 1.74 \pm 0.53 \times 10^{10} M_\odot$ and $M_s = 1.34 \pm 0.11 \times 10^{11} M_\odot$.

# 6 Conclusion

The obtained values for the baryonic mass and for the dark matter mass within $R_s$ are difficult to compare directly to published results, as the models in this paper are quite simplistic and the values obtained depend on the model used. Some comparison can be drawn from Robin et al. (2004) [3], which lists the mass of the central bulge, excluding the central black hole and clusters, as $M'_B = 2.03 \times 10^{10} M_\odot$, which relates to the $M_B$ parameter in this paper. The $M_s$ value can be compared based on Nesti, Salucci (2013) [4], which lists a value for the dark matter density $\rho_0 = 4 \times 10^7 M_\odot/\text{kpc}^3$. A reference for the $M_s$ parameter is obtained through Equation (7), $M'_s = 9.71 \times 10^{10} M_\odot$.

From comparison to the reference values in Figure 5, it is concluded that the approximation for baryonic mass $M_B$ is valid. However, there is a significant discrepancy between the obtained and reference values for $M_s$, which is a consequence of employing a simplified model in this paper. On the other hand, the reference $M'_s$, combined with the mass of the stellar thin disc $M_{td} = 2.15 \times 10^{10} M_\odot$ [3], which is the largest unaccounted contribution, gives a value much closer to the experimental result. Therefore it is concluded that the Model 2, while sufficient to model the acquired data within the experimental uncertainty, is too crude to accurately determine the mass of the dark matter, because the value obtained from it includes other contributions.

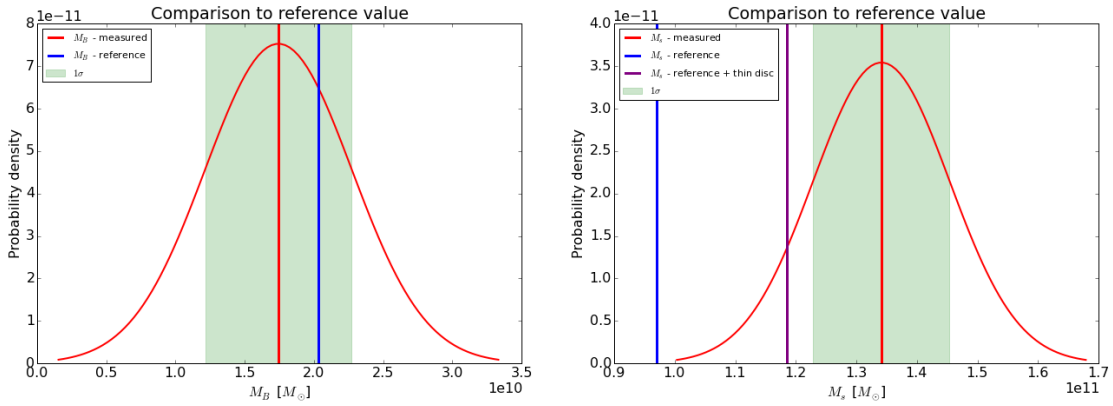


(a) $M_B$. (b) $M_s$.

Figure 5: Comparison to reference values.

This experiment suffers two main drawbacks; experimental uncertainty and simplicity of the models. The experimental uncertainty is quite large and could be improved by employing a radio telescope with better resolution. More importantly, the models considered are quite simple and even though Model 2 is successful in fitting the data, within the experimental uncertainty, it could be improved by including the contributions from the stellar thin disc, thick disc and interstellar matter.

# References


[1] J. Navarro, C. Frenk, S. White, *The Structure of cold dark matter halos*, The Astrophysical Journal 462, pp. 563-575. (1996).

[2] T. Piffl et al., *The RAVE survey: the Galactic escape speed and the mass of the Milky Way*, Astronomy and Astrophysics 562, pp. 91. (2014).

[3] A. Robin et al., *A synthetic view on structure and evolution of the Milky Way*, Astronomy and Astuophysics 416, pp. 157. (2004).

[4] F. Nesti,P. Salucci, *The Dark Matter halo of the Milky Way*, JCAP 1307, pp. 016. (2013).

[5] P. McMillan, *Mass models of the Milky Way*, Monthly Notices of the Royal Astronomical Society 414, p p. 2446-2457. (2011).

[6] J. Oort, *The Force exerted by the stellar system in the direction perpendicular to the galactic plane and some related problems*, Bulletin of the Astronomical Institutes of the Netherlands VI, pp. 249-287. (1932).

[7] J. Oort, *Measures of the 21-cm line emitted by interstellar hydrogen*, Vistas in Astronomy, vol. 1, Issue 1, pp.607-616 (1955).

[8] M. Higginson-Rollins, A. Rogers, *Development of a Low Cost Spectrometer for Small Radio Telescope (SRT), Very Small Radio Telescope (VSRT), and Ozone Spectrometer*, http://www.haystack.mit.edu/edu/undergrad/srt/pdf%20files/2013_HigginsonRollinsPaper.pdf. (Retrieved 5/1/2106).

[9] J. Binney, M. Merrifield, *Galactic Astronomy*, Princeton University Press, (1998).

[10] D. Marquardt, *An Algorithm for Least-Squares Estimation of Nonlinear Parameters*, SIAM Journal on Applied Mathematics 11 (2), pp. 431441. (1963).

# Appendix

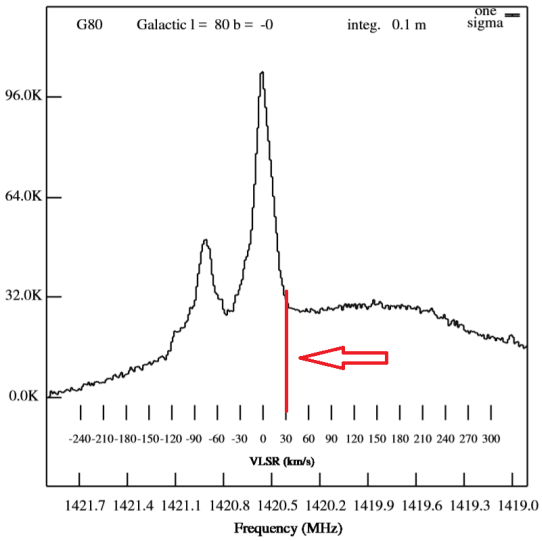


Figure 6: Measuring the relative velocity. A typical SRT output snapshot is shown. Here data was collected for 5 minutes at galactic longitude of 80°. The measurement is taken, where the source moves away the fastest, which corresponds to the inner-most orbit tangent to line of sight.

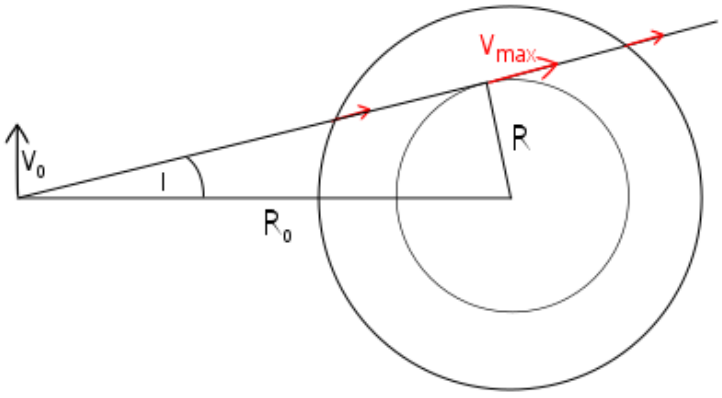


Figure 7: Obtaining rotational velocity. $v_{max}$ is the greatest measured $v_{LSR}$, which is shown in red.